

PAPER • OPEN ACCESS

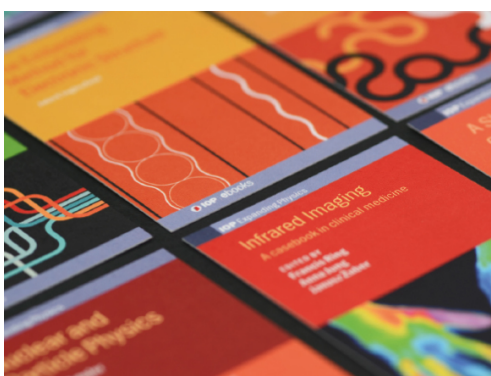
Hygrothermal simulations of timber-framed walls with air leakages

To cite this article: A Laukkarinen *et al* 2021 *J. Phys.: Conf. Ser.* **2069** 012094

View the [article online](#) for updates and enhancements.

You may also like

- [HAM Analysis of Selected Wooden-Framed Walls](#)
P Durica, V Kabatova, P Juras *et al.*
- [Practicability and reliability of direct component testing for in-situ measurement of building component airtightness](#)
M Prignon, A Dawans and G Van Moeseke
- [Thermal bridge occurrence in straw-bale timber frame walls](#)
P Brzyski, P Kosiski and M Nadratowska



IOP | ebooks™

Bringing together innovative digital publishing with leading authors from the global scientific community.

Start exploring the collection—download the first chapter of every title for free.

Hygrothermal simulations of timber-framed walls with air leakages

A Laukkarinen¹, T Jokela¹, T Moisio¹ and J Vinha¹

¹ Tampere University, Faculty of Built Environment, Civil Engineering, Building Physics, Tampere, Finland

anssi.laukkarinen@tuni.fi

Abstract. Air leakages can create substantial excess moisture loads into envelope structures and degrade their hygrothermal performance. Multiple previous research projects have studied the behaviour and modelling of air leakages in building physics applications, but it is still quite rare to see air leakages being considered in practical building design simulations. The purpose of this paper is to present the selection of input parameters for air leakage simulations, utilisation of a factorial design to manage simulation cases and the results for a timber-frame wall with and without air leakages. According to the results, the air permeability of mineral wool and the air pressure difference over the envelope were the two most important factors for the dry air mass flow through the structure, as opposed to gap width and leakage route. An ideally airtight structure had a better hygrothermal performance compared to leaky structure. However, when leakages were present, the exact yearly average air flow rate in the range 70...420 dm³/(m²h) did not have a strong correlation to the performance indicators. For the other studied variables, the existence of a 50 mm thick mineral wool insulation on the exterior side of the gypsum board wind barrier and the impacts from climate change had the biggest effect on the moisture performance of the structure.

1. Introduction

1.1. General

Air flows through building envelope structures can have negative effects on the hygrothermal performance of the structure, transport of impurities to indoor air, decrease thermal comfort and weaken the building energy performance. These impacts have been long identified and in many situations the research, guidelines and building practice related to building air tightness is in a better level nowadays compared to earlier decades.

At the same time it would be of interest to know, if there are some limits for air tightness values after which further improvements in the air tightness values start to get diminishing returns or there would be secondary effects e.g. with mechanical ventilation or fire safety. In general, air flow through envelope structures require air pressure difference over the envelope and some air permeable materials and/or leakage paths that allow air flow. The impacts from these air flows vary depending on the differences in building materials, details of the construction itself and on the building use.

The purpose of this paper is to present the selection of input parameters for air leakage simulations, test the use of factorial design to manage multiple simulation cases, and to present simulation results regarding the hygrothermal behaviour of timber-framed walls under air leakages.



1.2. Modelling of air flows through building envelope

In building physics applications, the two most implemented models for air leakages are the air change rate model and the Darcy's law. Air change rate model means here any simple sink/source term for air transfer, that could be calculated by hand. Air change rate is commonly (e.g. in Delphin [1] and WUFI [2]) used to take into account the impacts of intentional cavity ventilation in building components, but it has also been applied to create an effective moisture source [3] inside the simulated structures. In [3], a volumetric air flow rate is calculated as $q_{CL} = k_{CL} \cdot \Delta P$, where the reference value for k_{CL} is $7 \text{ dm}^3/(\text{m}^2\text{hPa})$. If we use a pressure difference of 10 Pa, the air flow rate can be calculated to be $7 \text{ dm}^3/(\text{m}^2\text{hPa}) * 10 \text{ Pa} = 70 \text{ dm}^3/(\text{m}^2\text{h})$. The air flow rate can then be used to calculate a moisture source into the structure.

Reference [4] uses equivalent leakage areas to describe the amount of air leakages through the envelope structure, for which the default values are $5.5\text{e-}6 \text{ m}^2/\text{m}^2$ for airtight building and $29\text{e-}6 \text{ m}^2/\text{m}^2$ for standard construction. These can be combined with the power law equation $q = C \cdot (\Delta p)^n$ [5, p. 16.15], and if we assume air pressure difference of 10 Pa and a discharge coefficient of $C_D = 1$, the equivalent leakage areas correspond to $81 \text{ dm}^3/(\text{m}^2\text{h})$ and $426 \text{ dm}^3/(\text{m}^2\text{h})$, respectively.

The power law can be also combined with the building air tightness value q_{50} , for which in Finland there is a minimum requirement of $4 \text{ m}^3/(\text{m}^2\text{h})$ for new construction. If we use a flow exponent of $n = 0.667$, then for a 10 Pa pressure difference the air flow rate through the envelope is: $q_{10} = 4 \text{ m}^3/(\text{m}^2\text{h}) * (10/50)^{0.667} = 1400 \text{ dm}^3/(\text{m}^2\text{h})$. For a pressure difference of 20 Pa the air flow rate is: $q_{20} = 4 \text{ m}^3/(\text{m}^2\text{h}) * (20/50)^{0.667} = 2200 \text{ dm}^3/(\text{m}^2\text{h})$. In these cases, the q_{50} value contains all leakages through the envelope and the leakages are distributed evenly throughout the envelope area. Earlier studies have shown however, that air leakage paths are strongly concentrated into different joints, which means that these areas can experience high-than-average air leakage rates, while the amount of air leakages in other envelope areas is small.

The Darcy's law describes a fully saturated laminar flow in porous medium and it is commonly used for building materials such as mineral wool to determine its' air permeability [6]. The rule-of-thumb limit for the applicability of Darcy's law is that the pore Reynolds number should be less than $1 \dots 10$. The Reynolds number for porous media can be calculated using permeability, such that: $Re_K = \rho v k^{0.5} / \mu$, where ρ is the fluid density (kg/m^3), v is the Darcy velocity (m/s), k is the permeability (m^2) and μ is the fluid dynamic viscosity ($\text{Pa}\cdot\text{s}$) [7]. If the permeability of mineral wool is in the range from $1.5\text{e-}9 \text{ m}^2$ to $6.0\text{e-}9 \text{ m}^2$, then the Darcy velocity should stay under $0.2 \dots 3.8 \text{ m}/\text{s}$ for the flow to be in the Darcy regime. For a 1 mm wide and 1 m long slit this would mean volumetric airflow rate between $680 \dots 14000 \text{ dm}^3/\text{h}$. The current version of SFS-EN 15026:2007 [8] does not include air flows through the structures.

Previous studies that have used simulations to study the impacts of air leakages on the heat and moisture performance of envelope structures include [9, 10, 11, 12, 13, 14, 15, 16]. In short, these studies have highlighted the importance and benefits of good building air tightness and the use proper thermal and vapour control layers to protect structures from moisture damages. Reductions in air leakages, adding thermal insulation on the exterior side of the main thermal insulation layer and ensuring good drying capabilities have all been considered beneficial for the hygrothermal performance of the envelope structures under air leakages. In [13], the impact from mineral wool permeability or leakage route arrangement on the amount of condensated moisture was small, whereas the pressure difference over the assembly was found to be the most important factor. An important notion from the previous results is that although air leakages can create significant risks to the moisture performance of assemblies, there are also multiple measures that can be taken to improve the fault-tolerance of the structures and even make them able to withstand limited amount of air leakages without deterioration.

2. Methods and materials for simulations

A timber-framed wall structure with a ventilated wooden cladding was studied. Two variants of the main structure were studied, where a) the wall had a 9 mm thick gypsum board as a wind barrier and

b) otherwise the same wall, but with a 50 mm thick mineral wool (MW) board with weather membrane on its exterior side. The structure in case a) is presented in figure 1 (left).

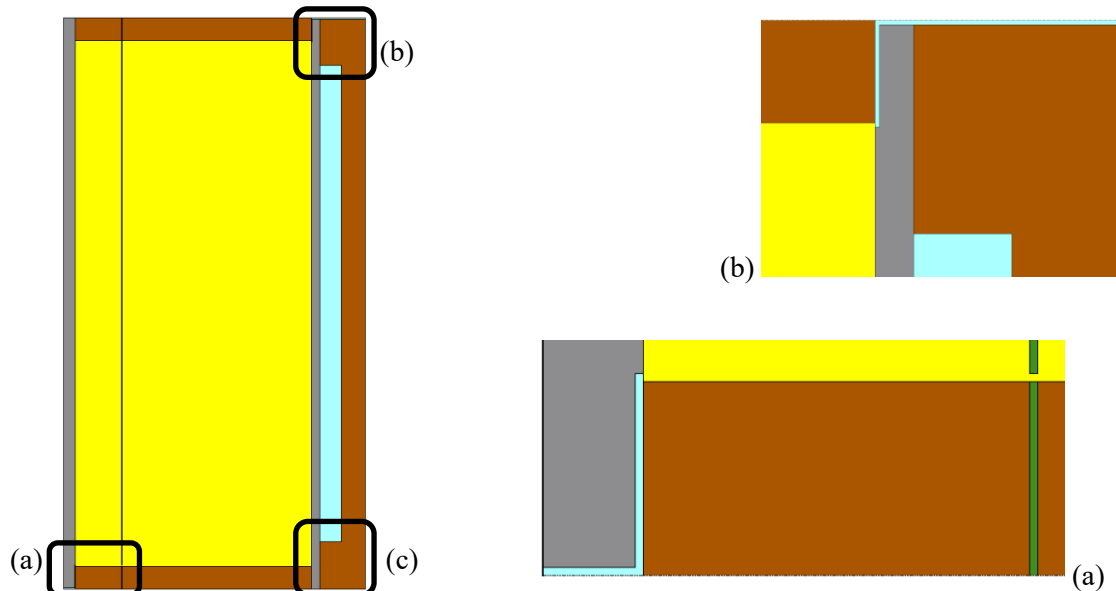


Figure 1. Left: The reference wall structure from top (indoors on the left). Right-bottom (a): L-shaped geometry of the inlet air gap. Right-top (b): L-shaped geometry of the outlet air gap at the adjacent wall stud. The outlet gap next to the inlet gap (c) was symmetrical to the adjacent stud outlet gap (b). The zoom level varies.

Air leakages were introduced into the model by adding small gaps next to the studs. On the interior side the gap was placed at the adiabatic border through the interior board and next to the short side of the wall stud then facing the mineral wool insulation. Another gap was placed into the air barrier right next to the wall stud. On the exterior side the gap was placed either next to the same wall stud than the gaps at the interior board and air/vapour barrier (shortest flow path) or next to the adjacent stud (longest flow path). In figure 1 (left), the inlets were at the bottom-left corner and the outlet either at the bottom-right or top-right corners of the structure. Wooden parts were made airtight. The gaps created a direct contact between indoor/outdoor air and the mineral wool insulation between the wall studs.

The building physical simulation tool Delphin 6.1 was used for the calculations. The simulations were run using a laptop computer and a Linux cluster Narvi maintained at Tampere University. To help replicability, the material properties were taken as directly as possible from the Delphin 6 material database. The material names and basic parameters are shown in Table 1. Anisotropic material properties were not included, because the current software version did not support them for air flows.

Table 1. Material names and basic properties used in the simulations.

| Name in Delphin 6 database | Basic material parameters | | | | | | | | |
|-----------------------------------|-----------------------------|----------------|-------------------------|--------------------------------------|---|--|---|------------------|------------------------|
| | ρ kg/m ³ | c_p J/kgK | λ_{dry} W/mK | μ - | θ_{80} m ³ /m ³ | θ_{eff} m ³ /m ³ | A_w kg/m ² s ^{0.5} | $K_{L,eff}$ s | K_a [5, 17, 18] s |
| Spruce_radial (from Saxony) [712] | 394 | 1840 | 0.112 | 186 | 0.060 | 0.729 | 0.012 | 1.81e-10 | Air tight |
| Mineral Wool [644] | 37 | 840 | 0.04 | 1 | 6.78e-5 | 0.9 | Water tight | | 1e-4, 2.5e-4 or 4e-4 |
| Gypsum board [81] | 850 | 850 | 0.2 | 10 | 0.0072 | 0.551 | 0.277 | 6.26e-9 | 8.6e-9 |
| PE-Foil [174] | 1500 | 2100 | 0.23 | Water tight, vapour tight, air tight | | | | | |
| DuPont Tyvek DPT [448] | 463 | 1000 | 0.23 | 519 | Foil | | 0.0001 | 1e-16 | 1e-8 |
| Air gap 25mm (vertical) [16] | 1.3 | 1050 | 0.138 | 0.4 | Air | | Water tight | | 0.1 |
| Air gap 03mm (vertical) [13] | 1.3 | 1050 | 0.03 | 1 | Air | | Water tight | | 0.1 |

For boundary conditions, two different situations were considered: First, constant one-week boundary conditions with 21°C, 50%RH and 101330 Pa for the indoor air and +5 °C, 80%RH and 101325 Pa for the outdoor air. These conditions were used to study the impact selecting different solvers, integrators and preconditions in Delphin 6 by looping through all the available combinations. The parameters for each of three choices were left to default.

Stationary conditions were used also to study the sensitivity of certain input parameters on the magnitude of dry air mass flux through the structure. A full factorial design with six factors and two levels for each (2^6 design, 64 cases) was done, where the factors and their levels were: leakage geometry (gaps next to same stud or adjacent studs), gap width (0.5 mm or 1 mm), number of elements in the gap (1 or 5), expansion factor for the automatic grid generation tool (1.3 or 2.0), air permeability of mineral wool (1.0e-4 s or 2.5e-4 s) and the air pressure difference over the envelope (10 Pa or 20 Pa). A time period of 6 h was simulated for each case and the dry air mass flux through interior gypsum board, gap in interior gypsum board, gap in air barrier, exterior gypsum board and gap in exterior gypsum board were recorded, along with the simulation time. The `statsmodels` Python package was used to fit an OLS regression model with interaction effects to the result data, where the categorical input variables were first coded to levels -1 and 1 and then all the input variables with constant term were scaled to the same range.

Second, two-year time-dependent simulations were done using hourly data from the Finnish building physical test years [19, 20]. In addition to previous boundary conditions, also solar radiation ($\alpha_{sol} = 0.6$), long-wave radiation and wind-driven rain was included. The building was assumed to be a two-storey (6 m high) building with even distribution of leakage routes in the envelope. The building was assumed to be located at SFS-EN ISO 15927-3:2009 [21] terrain category I, with $C_T = 1$, $O = 0.8$ and $W = 0.4$ for wind-driven rain calculations. The air pressure difference over the building envelope was calculated as the sum of thermal stack ($\Delta P_T = (gzP_e/R_a) \cdot (1/T_e - 1/T_i)$) and wind-dependent air pressure difference ($\Delta P_w = (c_{pi} - c_{pe}) \cdot (0.5\rho_a v^2)$). The air pressure difference from wind was calculated using a constant interior pressure coefficient $c_{pi} = -0.3$ and the SFS-EN 1991-1-4 exterior pressure coefficients for construction details [22], which were set to -0.5, +1.0 and -1.4 for wind blowing on the opposite side of the building, towards to studied façade and wind blowing from the side [16]. Similar ideas to factorial design were used here, but part of the cases was dropped to compensate for increased computational efforts. The input variables (factors) were: Gap width (0.5 mm or 1.0 mm), number of elements in the gap (1 or 5), air permeability of mineral wool (1.0e-4 s, 2.5 e-4 s or 4.0e-4 s), wall orientation (south or north), existence of additional 50 mm thick mineral wool insulation + weather membrane on the exterior side of wind barrier (yes or no), leakage route geometry (next to same studs or adjacent studs) and the choice of Finnish building physical test year (Jokioinen 2004, 2050 or 2100). Air leakages transported moisture into the structure. Results from the factorial design were not used to predict conditions for new situations.

The simulation results were analysed by visualisations (including interaction plots) and by calculating single-value indicators from the temperature (T) and relative humidity (RH) data. For each grid element in the stud and windbarrier surfaces facing the MW insulation, the yearly average T and RH were calculated, along with the hourly mould index M according to the Finnish mould growth model. From these, the minimum yearly average temperature, maximum yearly average relative humidity and maximum yearly mould index were selected for the two stud surfaces and the windbarrier surface. Finally, the order of importance of the input variables was determined by fitting a multiple linear regression model to the single-value indicator data (`statsmodels` OLS) and sorting the input variables according to the t-values of the model coefficients.

3. Results

3.1. Preliminary studies using stationary conditions

Regarding the simulation time, the fastest one was produced using the CVODE integrator, BiCGStab solver and ILU preconditioner. The next fastest simulation time was with the same integrator and

preconditioner, but with the GMRES solver. The combinations CVODE + KLU and ImplicitEuler + GMRES + ILU were also relatively fast. All the cases with the ExplicitEuler, ADI and RK integrators were slow or very slow. Other combinations were either somewhere in the middle of these two, were greyed out or didn't run. The automatic selector (Auto) selected typically GMRES + ILU combination, but also sometimes BiCGStab solver. Overall, it was concluded that the automatic preconditioner/solver/integrator selector worked quite well, but for larger sets of simulations it might be beneficial to test between GMRES and BiCGStab solvers. All the following results were calculated with the CVODE + BiCGStab + ILU combination. The dry air mass stayed the same between cases.

For the full hygrothermal simulations with air leakages, the air pressure difference for the first hour of the simulation was set to zero and the initial and minimum time steps were decreased, as this seemed to help for the simulation to start.

Table 2 shows the importance of different input parameters on dry air mass flux, determined by the t-values from the statsmodels OLS. The t-values were calculated for one model without interaction terms and one with interaction terms. The list contains also the group means when the sample (64 cases) was divided into two sets using each factor.

Table 2. The studied factors, their levels, the average dry air mass flux and the t-values for the regression model coefficients.

| Factor | t , no interactions | t , with interactions | Levels (low vs high) | Dry air mass flux (averaged over low and high levels) | Fold, high/low |
|--|---------------------|-----------------------|---|---|----------------|
| Air permeability of mineral wool | 20.6 | 4.4 | 1.0e-4 s vs 2.5e-4 s | 327 g/h vs 803 g/h | 2.46 |
| Air pressure difference over the structure | 16.3 | 3.1 | 10 Pa vs 20 Pa | 377 g/h vs 753 g/h | 2.00 |
| Gap width | 4.4 | 4.7 | 0.5 mm vs 1.0 mm | 514 g/h vs 616 g/h | 1.20 |
| Leakage route | 2.8 | 4.0 | Gaps next to adjacent studs vs same stud | 533 g/h vs 597 g/h | 1.12 |
| Number of elements in gap | 1.3 | 2.0 | 1 vs 5 (1 mm vs 0.2 mm or 0.5 mm vs 0.1 mm) | 550 g/h vs 580 g/h | 1.06 |
| Expansion factor | 0.6 | 1.1 | 2.0 vs 1.3 | 558 g/h vs 572 g/h | 1.03 |

The two most important parameters on the dry air mass flux were the air permeability of mineral wool and the pressure difference over the envelope, whereas the details of the calculation grid had a smaller impact on the results. The dry air mass flow rate increased linearly as a function of air pressure difference, which was opposed to the presumption of power law type behaviour and possible nonlinear effects from two-dimensional geometry. The results showed interactions between air permeability and pressure difference (stronger interaction), and between the gap arrangement and gap width (weaker interaction), which were likely the cause for the high t-values for air permeability of mineral wool and air pressure difference in the no-interactions model. The existence of interactions mean that specifying the numerical value of just one factor (e.g. air pressure difference) doesn't uniquely determine the dry air mass flow rate through the structure.

The dry air mass flow rates were in the range 201–1298 g/h for the gaps next to the same wall stud, and 182–1141 g/h for gaps being next to adjacent studs. If these values are divided by air density 1.25 g/dm³ and wall section area of 0.6 m², we get volumetric air flow rates of 270–1700 dm³/(m²h) and 240–1500 dm³/(m²h), respectively. These values can be considered to be somewhat in line with the literature values presented in Ch. 1.2, but the uncertainties related to them are high.

The yearly average air velocity at the air barrier gap was 0.01–0.1 m/s and significantly lower further away from it. For these values the pore Reynolds number was in most of the cases higher than 1–10, which would imply that the flow would not be in the Darcy's law range in the small gap area, and could explain the power law type air flow behaviour measurements of full structures and buildings. The air flow through the gypsum boards was small (0.01 % – 1.3 %) compared to the air flow through the gaps, i.e. gaps dominated the flow paths compared to flow through gypsum boards.

3.2. Simulation results for building physical test year conditions

The gap width and the number of elements in the gap showed strong multicollinearity related to the full-year simulations, which caused high condition numbers in the OLS regression. This was dealt with by simply removing the minimum element size from the OLS input parameters.

Table 3 shows the t-values for the multiple linear regression model coefficients. The number of simulations was 108, which was a reduced value compared to a full factorial design. The simulation models in this chapter included all climatic variables.

Table 3. t-values for the multiple linear regression coefficients when each of the output variables ($j_{m,a}$, RH, T, M) are analysed separately. The models included interaction effects.

| Factor | Air barrier, gap $j_{m,a}$ | Wind barrier, against MW | | | Stud long edge, fig. 1 bottom | | | Stud long edge, fig. 1 top | | | Average t-values | | | |
|-------------|----------------------------------|-----------------------------|-------|------|----------------------------------|-------|------|-------------------------------|------|-------|------------------|-------|------|-------|
| | | RH | T | M | RH | T | M | RH | T | M | RH | T | M | All |
| 50 mm MW | 0.33 | 5.19 | 8.81 | 6.95 | 6.09 | 8.09 | 4.27 | 14.24 | 9.31 | 15.53 | 8.51 | 8.74 | 8.92 | 8.72 |
| Climate | 0.96 | 2.71 | 47.86 | 5.88 | 4.27 | 36.74 | 2.25 | 9.16 | 42.4 | 7.71 | 5.38 | 42.33 | 5.28 | 17.66 |
| Same/adjct | 0.99 | 2.12 | 0.34 | 1.11 | 0.27 | 0.84 | 2.51 | 8.32 | 2.03 | 2.27 | 3.57 | 1.07 | 1.96 | 2.20 |
| Orientation | 4.28 | 0.23 | 2.24 | 1.26 | 0.16 | 3.42 | 0.66 | 1.7 | 3.08 | 3.47 | 0.70 | 2.91 | 1.80 | 1.80 |
| Kg of MW | 3.58 | 1.87 | 0.26 | 0.28 | 1.86 | 1.14 | 0.09 | 3.18 | 0.24 | 0.29 | 2.30 | 0.55 | 0.22 | 1.02 |
| Gap width | 0.18 | 3.56 | 0.06 | 0.32 | 2.92 | 0.78 | 0.34 | 0.15 | 0.02 | 0.41 | 2.21 | 0.29 | 0.36 | 0.95 |

It was noticed that the order of variable importance varied depending on what output variable was used for the regression model and if the regression coefficients or their t-values were used for ranking. There were also cases, where two variables by themselves were not significant, but their interaction was. The data was analysed further with statsmodels interaction plots which showed that there were multiple interactions and nonlinearities present in the data. Physical explanations could be given to some of these, such as the boundedness of mould index, step-wise change in conditions when air leakages were present (figure 2), accelerating change in moisture conditions due to climate change and a big categorical change in conditions when additional exterior mineral wool insulation was present. A good side was that in many cases the interaction effects could be predicted from the main effects (Table 3). The impacts of air leakages are studied further in figure 2.

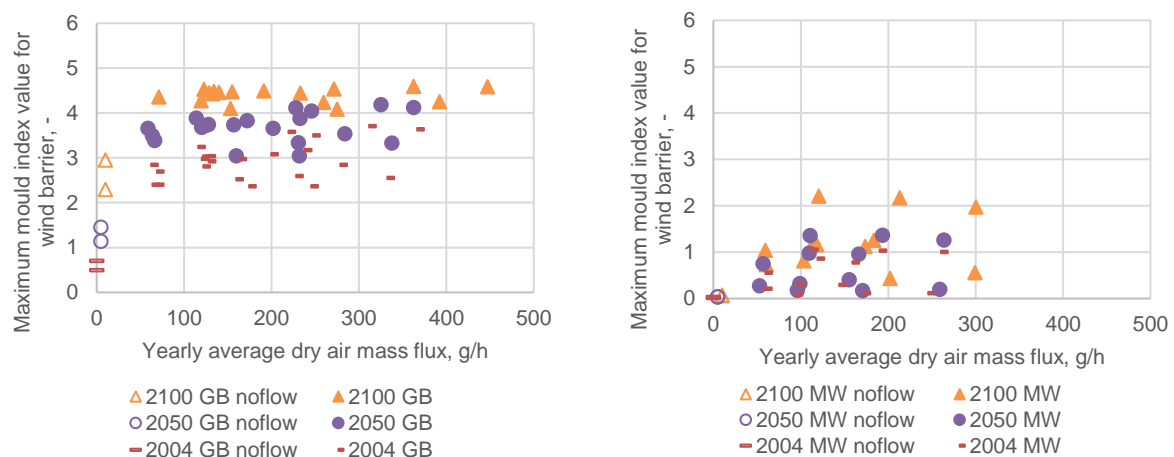


Figure 2. The maximum mould index value in the interior surface of the gypsum board (GB) wind barrier as a function of the dry air mass flux through the structure without (left) or with (right) additional thermal insulation (MW). The left-most values are given a small horizontal displacement to show them better.

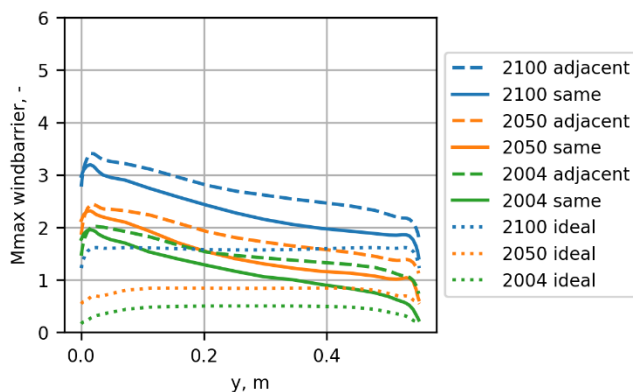


Figure 3. Maximum mould index at the interior surface of wind barrier.

leakage path, the most critical point in the wind barrier was right in front of the inlet gap (also from the wooden stud perspective). The longer air flow path was more critical compared to the shorter flow route. The wooden studs acted as thermal bridges and decreased the M_{max} values in the wind barrier at the short (< 1 cm) length close to the studs.

The existence of additional 50 mm mineral wool insulation was one of the main factors affecting the conditions inside the structure. Climate change had also a big negative impact on the performance indicators. Air leakages weakened the performance of the structure, especially when there were no additional exterior thermal insulation present. The wall orientation, air permeability of mineral wool and leakage arrangement seemed to have some impacts on the results, but mainly through interactions with other variables. Impacts from gap width were modest in preliminary studies, but more pronounced in the full hygrothermal simulations. The role of wall orientation was pronounced from temperature perspective, which was likely due to the changes in solar radiation to the surface.

4. Conclusions

This study conducted a series of hygrothermal simulations to study the behaviour and impacts of air leakages in a timber-frame wall. The ideas from factorial design were used to manage and analyse the simulation cases, so that as much information as possible could be extracted from a finite set of simulations. The simulations did not consider three-dimensional flow paths, anisotropic material properties, limitations to using Darcy's law or many other topics, such as speed of moisture sorption.

Using a factorial design was considered helpful in managing a small group of simulations and in highlighting the existence of numerous interactions and nonlinearities between variables in coupled HAM problems. The analysis of data with interaction terms was also a challenge, because the physical background for the interaction terms or variable importance was not always clear.

The dry air mass flux through the structure happened almost completely through the small gaps introduced into the geometry, whereas the flow through the interior and exterior gypsum boards was small in comparison. The two most influential factors for dry air mass flow were the air permeability of mineral wool and air pressure difference, whereas the gap width and details of the discretisation grid had a smaller impact.

From the viewpoint of moisture performance of the structure, the most influential factor was that of having a 50 mm thick mineral wool insulation on the exterior side of the gypsum board wind barrier. The predicted climate change also caused a significant impact on the hygrothermal performance of the structure. The wall orientation and geometrical arrangement of air leakages had a noticeable effect, but smaller compared to the two previous ones. Air flows into the structure weakened the moisture performance of the structure and the most beneficial situation was to not have any air leakages at all. However, when air leakages were present, their exact amount ($70\text{--}420$ $\text{dm}^3/(\text{m}^2\text{h})$) did not have a clear correlation to the moisture behaviour of the structure.

References

- [1] Delphin 2021 Simulation program for the calculation of coupled heat, air, moisture, pollutant and salt transport, <https://www.bauklimatik-dresden.de>
- [2] WUFI 2021, Building component simulations (WUFI Pro and WUFI 2D), <https://wufi.de/en/>
- [3] WTA Merkblatt 6-2. 12.2014/D 2014 Simulation of Heat and Moisture Transfer
- [4] ASHRAE 160 2016 Criteria for Moisture-Control Design Analysis in Buildings
- [5] ASHRAE, ASHRAE Fundamentals, 2017.
- [6] SFS-EN ISO 9053-1:2018, Acoustics. Determination of airflow resistance. Part 1: Static airflow method
- [7] Nield D, Bejan A 2017 Convection in Porous Media, 5th ed., Springer International Publishing
- [8] SFS-EN 15026:2007 Hygrothermal performance of building components and building elements. Assessment of moisture transfer by numerical simulation
- [9] Ojanen T, Simonson C 1992 Convective moisture accumulation in structures with additional inside insulation, *Thermal Envelopes VI*, Clearwater Beach, Florida
- [10] Janssens A, Hens H 2003 Interstitial Condensation Due to Air Leakage: A Sensitivity Analysis, *J. of Thermal Env. & Bldg. Sci.* 27 (1), pp. 15-29
- [11] Kalamees T and Kurnitski J 2010 Moisture Convection Performance of External Walls and Roofs, *J Build Phys* 33 (3), pp. 225-247
- [12] Kosinski P, Brzyski P, Suchorab S and Lagod G 2020 Heat Losses Caused by the Temporary Influence of Wind in Timber Frame Walls Insulated with Fibrous Materials, *Materials* 13 (23)
- [13] Kölsch P, Zirkelbach D, Nusser B, Wagner R, Zegowitz A and Künzel H 2016 Airflow through Lightweight Wall Assemblies - Influence of Size and Location of Leakages, *Buildings XIII Conference. Clearwater Beach, Florida*, pp. 459-484
- [14] Bednar T, Deseyve C, Jung M, Nusser B and Teibinger M 2010 Impact of Airflow on the Risk Assessment of Flat Roofs, *IAQVEC 2010, Syracuse, New York.*, 8 p.
- [15] Jokela T 2018 Hygrothermal Performance of Timber-Framed External Walls with Gypsum Board Sheathing, M.Sc. thesis. <http://urn.fi/URN:NBN:fi:tty-201811262762> [In Finnish]
- [16] Moio T 2020 Hygrothermal performance of timber-framed external wall junctions. M.Sc. thesis. <http://urn.fi/URN:NBN:fi:tuni-202005255628> [In Finnish]
- [17] Hurel N, Pailha M, Garnier G and Woloszyn M 2017 Impact of different construction details on air permeability of timber frame wall assemblies: Some experimental evidence from a three-scale laboratory study, *J Build Phys*, 41(2), pp. 162-189.
- [18] Knauf 2014 Weatherboard. Product data sheet. 9GM-H1, Espoo, Finland.
- [19] Vinha J, Laukkarinen A, Mäkitalo M, Nurmi S, Huttunen P, Pakkanen T, Kero P, Manelius E, Lahdensivu J, Köliö A, Lähdesmäki K, Piironen J, Kuhno V, Pirinen M, Aaltonen A and Suonketo J 2013 <http://urn.fi/URN:ISBN:978-952-15-2949-8>, [In Finnish]
- [20] Ruosteenoja K, Jylhä K, Mäkelä H, Hyvönen R, Pirinen P and Lehtonen I 2013 <http://hdl.handle.net/10138/38648> [In Finnish]
- [21] SFS-EN ISO 15927-3 2009 Hygrothermal performance of buildings - Calculation and presentation of climatic data - Part 3: Calculation of a driving rain index for vertical surfaces from hourly wind and rain data
- [22] SFS-EN 1991-1-4 + AC + A1 2011 Eurocode 1: Actions on structures. Part 1-4: General actions. Wind actions.